

## **Time Variability of Molecular Line Emission in IRC+10216**

D. Teyssier<sup>1</sup>, J. Cernicharo<sup>2</sup>, G. Quintana-Lacaci<sup>2</sup>, M. Agúndez<sup>2</sup>, M.J. Barlow<sup>3</sup>, F. Daniel<sup>4</sup>, E. de Beck<sup>5</sup>, L. Decin<sup>6</sup>, P. Garcia Lario<sup>1</sup>, M.A.T. Groenewegen<sup>7</sup>, D.A. Neufeld<sup>8</sup>, J.C. Pearson<sup>9</sup>

<sup>1</sup>*ESAC/ESA, P.O. Box 78, E-28691 Villanueva de la Cañada, Madrid, Spain*

<sup>2</sup>*ICMM/CSIC, E-28049 Cantoblanco, Madrid, Spain*

<sup>3</sup>*University College London, Gower Street, London WC1E 6BT, UK*

<sup>4</sup>*IPAG, CNRS UMR5571, B.P. 53, 38041 Grenoble Cedex 09, France*

<sup>5</sup>*MPIfR, Auf dem Hügel 69, 53121, Bonn, Germany*

<sup>6</sup>*Instituut voor Sterrenkunde, KUL, B-3001 Leuven, Belgium*

<sup>7</sup>*Royal Observatory of Belgium, B-1180 Brussels, Belgium*

<sup>8</sup>*The Johns Hopkins University, Baltimore, MD, 21218, USA*

<sup>9</sup>*JPL, California Institute of Technology, Pasadena, CA, 91109, USA*

**Abstract.** We present the results of a monitoring of the molecular emission in the C-rich AGB star IRC+10216 over 3 years with the Herschel Space Observatory. Rotational transitions of various vibrational levels of CO, <sup>13</sup>CO, CS, CCH, H<sub>2</sub>O, SiO, SiS, SiC<sub>2</sub>, HCN and HNC have been collected with the HIFI, PACS and SPIRE instruments over multiple epochs. The intensity monitoring shows strong and periodic variations of most of the observed molecules, often with differential behaviour depending on the transition level (larger variation at higher J), and generally enhanced oscillation in the vibrational modes of some of these molecules (e.g. HCN). These results show that the effect of IR pumping through the different vibrational levels on the emergent line profiles of a given transition can be really significant. This implies that the IR radiation field of circumstellar envelopes and its time variation has to be taken into account in any radiative transfer model in order to derive accurate physico-chemical structure of the envelope.

### **1. Introduction**

IRC+10216 (CW Leo), like all Mira-type stars, shows significant amplitude modulation in the visible and the IR (e.g. 2 mag in the I band over a period of 635 days, Alksnis 1989). However, variation in the rotational levels of many of the molecular species present in the envelope (excited mainly through collision) was shown to be negligible, especially in the outer shell which is probed at millimetre wavelengths (Cernicharo, Guélin & Kahane 2000). Observations of thermal lines with the Herschel Space Observatory, however, revealed significant intensity variations on a 6 month time interval, that could not be explained by instrumental effects. Noteworthy, some other species

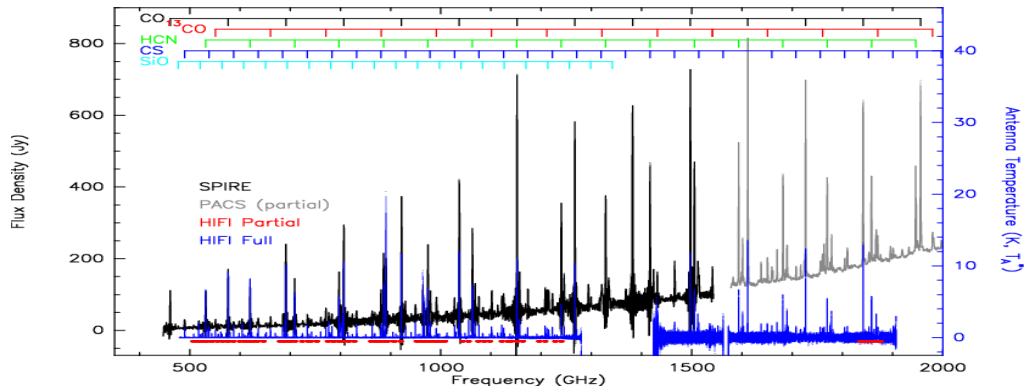


Figure 1. Example of a set of data collected at one given epoch. The HIFI data in blue correspond to the full spectral scan (Cernicharo et al. 2010), while the red portion correspond to the part of the spectrum regularly monitored. The PACS data are only shown in the range overlapping with HIFI, but they extend down to  $70 \mu\text{m}$ . The frequency of typical line ladders are indicated on the upper part of the plot.

like  $\text{SiC}_2$  (Cernicharo et al. 2010) did not show any noticeable variation. This motivated the monitoring of nearly a hundred of spectral line transitions for the remainder of the *Herschel* mission. We present here the data obtained in this context and highlight some of the early results.

## 2. Data-set acquisition and data analysis

The data-set consists of multi-epoch observations of large portion of the submm and FIR spectrum of IRC+10216 using the three spectrometers on-board *Herschel*. Full range spectroscopy was obtained with both PACS (Poglitsch et al. 2010) and SPIRE (Griffin et al. 2010) at 7 and 8 epochs respectively, stemming both from our monitoring programme and from regular instrumental calibration campaigns. For HIFI (de Graauw et al. 2010), dedicated tuning observations were performed to monitor  $\sim 80$  thermal lines over the 14 bands offered by the instrument. Additional measurement points were obtained from two other studies of this object (Cernicharo et al. 2010, Agúndez et al. 2011), providing in total 7 epochs for HIFI.

Fig. 1 illustrates the typical set of data obtained for a given epoch. For each epoch and spectral range, the source continuum was estimated and isolated from the spectral line emission (for HIFI no significant continuum emission was detected so the overall baseline level was simply subtracted). For each line and epoch, integrated line intensities were computed. For PACS and SPIRE, lines are spectrally unresolved so a Gaussian or Cardinal sine functions were respectively fitted at the expected line positions. For HIFI, spectrally resolved profiles cannot be fitted with a simple function due to the complex velocity structure. Line fluxes were integrated within predefined velocity windows. The collection of line fluxes at various epochs provides a light-curve that is then fitted with a simple sine function where amplitude, phase, period and average flux are considered free parameters. This approach is similar to the analysis of light-curves in the visible and NIR (e.g. Menten et al. 2012). Fig. 2 shows the typical outcome of this fitting exercise over a collection of HCN transitions measured by PACS.

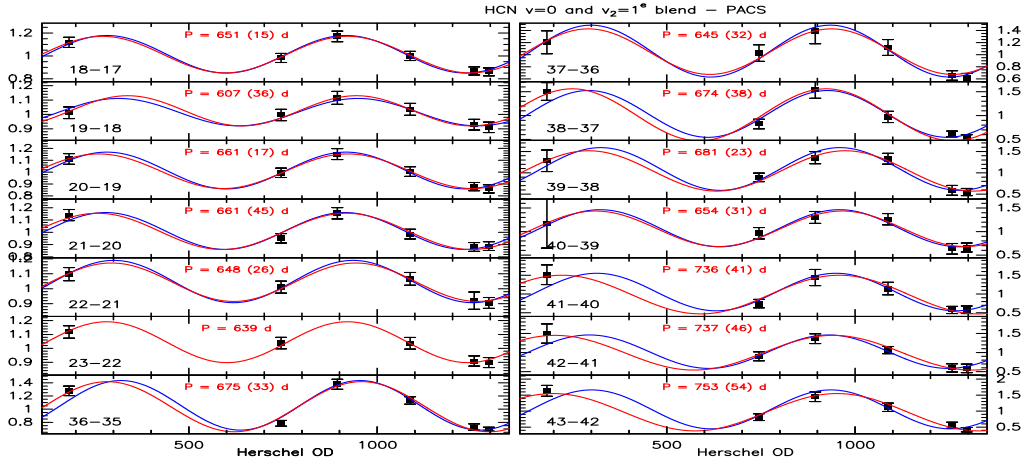


Figure 2. Example light-curves of integrated line intensity of the HCN ladder in the PACS spectral range. Intensities are normalised to the mean. A sine wave fit with a fixed period of 635 days is shown in blue, while the full-free parameter fit is shown in red, together with the fitted period in days in each box. The time axis is given on a scale of *Herschel* Observational Day (OD) – OD 1 is 14-May-2009.

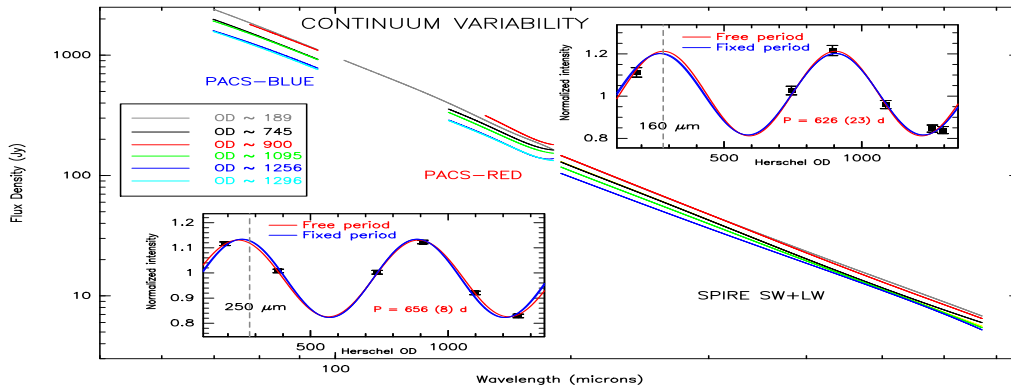


Figure 3. PACS and SPIRE continuum SED extracted at various epochs. Fit to the continuum light-curves at two wavelengths are given in the two insets, together with the fitted epochs in days. The vertical dashed lines there shows the position of the maximum of light fitted by Groenewegen et al. (2012) on SPIRE photometer data at 250  $\mu\text{m}$ .

### 3. Continuum variability

Using the continuum Spectral Energy Distribution (SED) isolated from the line emission, it is possible to create light-curves at any wavelength and fit them with a sine function. Fig. 3 shows an example of the fitted modulation at two wavelengths falling in the respective PACS and SPIRE ranges. The modulation fitted at 250  $\mu\text{m}$  is consistent with that derived by Groenewegen et al. (2012) using the SPIRE photometer. While the fitted period does not vary too much with the wavelength, the amplitude of the modulation tends to increase with decreasing wavelength, ranging typically from 25% at 600  $\mu\text{m}$  to more than 50% at 80  $\mu\text{m}$ .

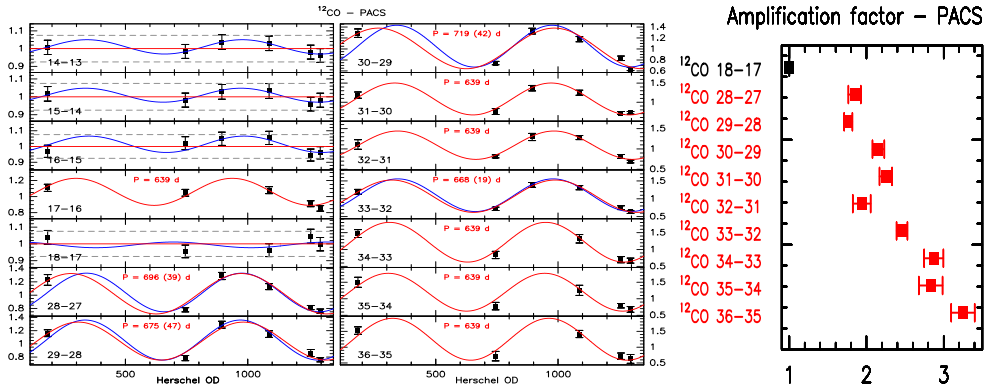


Figure 4. *Left*: Same as Fig. 2 for the CO ladder. Horizontal dashed lines indicate the range of intensity calibration uncertainty. For the  $J=17-16$  transition, a blend with an HCN  $\nu_1=1$  line exists, leading to the large modulation. *Right*: Amplitude modulation factor as function of rotational level for the higher range of the PACS data. The  $J=18-17$  transition, interpreted to be unmodulated, is shown in black.

#### 4. CO line variability

The analysis of CO line is probably the most widely-used tool to measure the main properties of circumstellar envelopes around AGB stars, and in particular to derive mass-loss rates. With the advent of detector and telescope technology, transitions of higher excited lines have been progressively added to such analysis, allowing to probe the emission in more internal layers of the envelope and constraint e.g. the gas temperature profile more precisely (e.g. de Beck et al. 2012). Such study, however, usually rely on a plethora of data collected over various telescopes and epochs, so they intrinsically assume that the CO line emission is not varying with time. Our data-set suggests that this assumption is fine typically up to rotational levels in the range  $J = 13$  to  $J = 18$ . In this range however, the modulation is within or only marginally above the typical instrument calibration errors so it is difficult to draw firm conclusion (see e.g. the left panels of Fig. 4). When one gets to rotational levels in the higher PACS frequency range ( $J = 28$  and above) amplitude modulations of a factor of 2-3 are observed, and tend to scale together with the upper energy level (see right panel of Fig. 4).

#### 5. Infrared Pumping

HCN lines in various vibrational states have been detected for several rotational transitions. The high spectral resolution of HIFI allows to separately analyse lines from  $\nu=0$  (ground-state),  $\nu_1=1$  and  $\nu_3=1$  (stretching modes with rotational ground-states lying at 3 and 4.8  $\mu\text{m}$  respectively), and  $\nu_2=1^e$ ,  $\nu_2=1^f$  and  $\nu_2=2$  (bending mode comprising an  $l$ -type doubling and the first overtone, with rotational ground-states lying at 14 and 7  $\mu\text{m}$  respectively). For PACS and SPIRE data, line blends occur between respective transitions of the  $\nu=0$  and  $\nu_2=1^e$  modes, and the  $\nu_2=1^f$  and  $\nu_2=2$  modes. Fig. 2 and 5 illustrate the light-curves of several of these transitions for PACS and HIFI data, together with their sine fit (see caption for further details). The right panel of Fig. 5 shows the evolution of fitted amplitude modulation factor at different rotational levels, and for the various vibrational modes. A clear trend is observed, whereby the amplitude of the

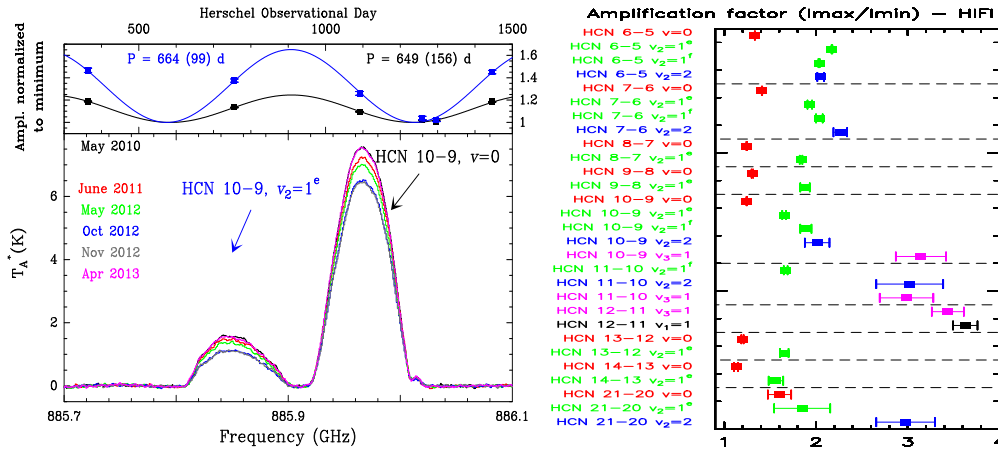


Figure 5. *Left*: Example of HCN spectra detected with HIFI. The lower panel show the respective spectra observed at different epochs. The upper inset shows the light-curves of the integrated intensities and their fit with a sine function, together with the fitted epoch in days. *Right*: Amplitude modulation factor for various vibrational modes and rotational levels for all HCN lines detected with HIFI.

modulation increases progressively from the ground-state to the bending modes, then to the two stretching modes, in line with the progressively increasing energy levels associated to the respective rovibrational transitions. Considering the high energy levels involved, collisional pumping is unlikely so that radiative pumping must be invoked. Because the corresponding wavelengths are probably very close to those where the star flux experiences the largest amplitude modulation, the effect we observe here should be a direct consequence of infrared pumping of the rovibrational transitions.

A similar effect is evidenced in the emission of the  $C_2H$  molecule. This latter exhibits the largest amplitude modulation of the whole sample (factor in excess of 10 for the  $N=7-6$  and  $N=8-7$  transitions). De Beck et al. (2012) already reported the importance of including the first three vibrational modes to reproduce the observed line intensities in the HIFI range. Once again, the radiative pumping involved occurs at wavelengths ( $3-27 \mu m$ ) where the star flux experiences large variation. On top of that, the first stretching mode of  $C_2H$  is coupled to the first electrically excited state ( $A\Pi^2$ ), lying at  $2.5 \mu m$ . All this shows that the infrared radiation field of circumstellar envelopes, and its time variation, has to be taken into account in radiative transfer models, in order to derive accurate physico-chemical structure of the shell.

## References

- Agúndez, M., Cernicharo, J., Waters, L.B.F.M., et al., 2011, *A&A* 533, L6  
 Alksnis, A., 1989, *Information Bulletin on Variable Stars*, 3315, 1  
 de Beck, E., Lombaert, R., Agúndez, M., et al., 2012, *A&A* 539, A108  
 Cernicharo, J., Guélin, M., Kahane, C., 2000, *A&AS* 142, 181  
 Cernicharo, J., Waters, L.B.F.M., Decin, L., et al., 2010, *A&A* 521, L8  
 de Graauw, Th., Helmich, F.P., Phillips, T.G., et al., 2010, *A&A* 518, L6  
 Griffin, M.J., Abergel, A., Abreu, A., et al., 2010, *A&A* 518, L3  
 Groenewegen, M.A.T., Barlow, M.J., Blommaert, J.A.D.L., et al., 2012, *A&A* 543, L8  
 Menten, K.M., Reid, M.J., Kamiński, T., et al., 2012, *A&A* 543, A73  
 Poglitsch, A., Waelkens, C., Gies, N., et al., 2010, *A&A* 518, L2